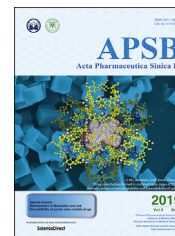




Chinese Pharmaceutical Association
Institute of Materia Medica, Chinese Academy of Medical Sciences

Acta Pharmaceutica Sinica B

www.elsevier.com/locate/apsb
www.sciencedirect.com



ORIGINAL ARTICLE

Reprogrammed siTNF α /neutrophil cytopharmaceuticals targeting inflamed joints for rheumatoid arthritis therapy

Yijun Chen[†], Kaiming Li[†], Mengying Jiao[†], Yingshuang Huang,
Zihao Zhang, Lingjing Xue, Caoyun Ju*, Can Zhang*

State Key Laboratory of Natural Medicines, Jiangsu Key Laboratory of Drug Discovery for Metabolic Diseases,
Center of Advanced Pharmaceuticals and Biomaterials, China Pharmaceutical University, Nanjing 210009, China

Received 22 April 2022; received in revised form 4 July 2022; accepted 20 July 2022

KEY WORDS

Neutrophil
cytopharmaceuticals;
siRNA;
Macrophages;
Rheumatoid arthritis;
Tumor necrosis factor α ;
Gene delivery;
Anti-inflammatory;
Cartilage protection

Abstract Rheumatoid arthritis (RA) is an autoimmune disease characterized by severe synovial inflammation and cartilage damage. Despite great progress in RA therapy, there still lacks the drugs to completely cure RA patients. Herein, we propose a reprogrammed neutrophil cytopharmaceuticals loading with TNF α -targeting-siRNA (siTNF α) as an alternative anti-inflammatory approach for RA treatment. The loaded siTNF α act as not only the gene therapeutics to inhibit TNF α production by macrophages in inflamed synovium, but also the editors to reprogram neutrophils to anti-inflammatory phenotypes. Leveraging the active tendency of neutrophils to inflammation, the reprogrammed siTNF α /neutrophil cytopharmaceuticals (siTNF α /TP/NEs) can rapidly migrate to the inflamed synovium, transfer the loaded siTNF α to macrophages followed by the significant reduction of TNF α expression, and circumvent the pro-inflammatory activity of neutrophils, thus leading to the alleviated synovial inflammation and improved cartilage protection. Our work provides a promising cytopharmaceutical for RA treatment, and puts forward a living neutrophil-based gene delivery platform.

© 2022 Chinese Pharmaceutical Association and Institute of Materia Medica, Chinese Academy of Medical Sciences. Production and hosting by Elsevier B.V. This is an open access article under the CC BY-NC-ND license (<http://creativecommons.org/licenses/by-nc-nd/4.0/>).

*Corresponding authors. Tel./fax: +86 25 83271171 (Can Zhang), +86 25 83271076 (Caoyun Ju).

E-mail addresses: jucaoyun@cpu.edu.cn (Caoyun Ju), zhangcan@cpu.edu.cn (Can Zhang).

[†]These authors made equal contributions to this work.

Peer review under responsibility of Chinese Pharmaceutical Association and Institute of Materia Medica, Chinese Academy of Medical Sciences.

<https://doi.org/10.1016/j.apsb.2022.08.012>

2211-3835 © 2022 Chinese Pharmaceutical Association and Institute of Materia Medica, Chinese Academy of Medical Sciences. Production and hosting by Elsevier B.V. This is an open access article under the CC BY-NC-ND license (<http://creativecommons.org/licenses/by-nc-nd/4.0/>).

1. Introduction

Rheumatoid arthritis (RA) is an autoimmune disease dominated by synovitis of unknown etiology, which affects about 1% of the world's population and is one of the most common chronic inflammation disease¹. The typical characterization of RA is the massive infiltration of immune cells (such as macrophages, neutrophils and so on) at joint synovial, which further produce large amounts of inflammatory cytokines, leading to severe synovial inflammation, cartilage damage, progressive disability, and even premature death, accompanying with socioeconomic burdens^{2,3}. Of which, tumor necrosis factor α (TNF α) overexpressed by macrophages in the inflamed synovium, plays a central role in RA advancement^{4–6}. TNF α can not only support its role in inflammation and affect cartilage cell metabolism, but also promote the secretion of other inflammatory mediators, such as interleukin (IL)-1, IL-6, and granulocyte-macrophage colony-stimulating factor (GM-CSF), forming a complex inflammatory network which potentiates the inflammatory response^{5–8}. The pathological inflammatory microenvironment comprising multiple immune cells and various inflammatory factors make RA hard to cure^{9,10}. Although anti-TNF- α antibody can inhibit the TNF α action effectively, and thereby attune the synovial inflammation and retard joint damage, there are almost 40% of non-responders to this anti-TNF- α treatment, usually accompanying with various side effects¹¹. Moreover, long-term use of anti-TNF- α antibody is costly¹¹. The commonly used drug, methotrexate (MTX), can only inhibit inflammation and alleviate pain of RA patients, but cannot halt or reverse disease progression^{12–16}, which either accompanies with some serious side effects such as hepatotoxicity, leading to the high withdrawal ratio⁴. Hence, development of alternative treatments that overcome the complex inflammatory network especially the pro-inflammation effect of TNF α is urgently needed for effective RA treatment.

Neutrophils are one of the most abundant leukocytes in peripheral blood. Their responsibility is to eliminate the foreign pathogen through phagocytosis, degranulation and the formation of neutrophil extracellular traps (NETs) in the inflammatory sites¹⁷. The representative inflammatory chemotaxis of neutrophils makes them able to firstly reach the inflammatory tissue, such as the inflamed joints¹⁸. Moreover, neutrophils play an important role in resolving inflammation and repairing tissue damage. For example, the neutrophil-derived microvesicles have been demonstrated to protect the cartilage and joint in RA^{19,20}. And the neutrophil membrane can bind with inflammatory cytokines either, which can neutralize the inflammatory response and thus protecting the cartilage^{19,20}. Leveraging these merits, neutrophils could serve as alternative drugs for RA therapy. However, the ability of neutrophils to initiate and perpetuate RA progression²¹ through releasing higher levels of TNF α ^{19,22}, has restricted their application. Therefore, reprogramming neutrophils with the down-regulation of TNF α might be potential in RA therapy.

Small interfering RNAs (siRNA) that can silence the specific messenger RNA (mRNA) as well as its downstream protein, has been confirmed as a safe and efficient gene drug. With the recent FDA approval of the first siRNA-derived therapeutic (Onpatro), RNA interference (RNAi)-mediated gene therapy is undergoing a transition from research to the clinical space²³. Using TNF α -targeting siRNA (siTNF α) to selectively suppress the production of the pro-inflammatory TNF α cytokine in neutrophils could be a suitable approach to reprogram neutrophils.

In addition, if high levels of TNF α produced by macrophages in inflamed joints are suppressed by siTNF α , could further regulate the

inflammatory network, alleviate the inflammation, and thus avoiding the cartilage destruction^{24–27}. However, the delivery of siTNF α to macrophages in RA joints still faces great challenges^{28,29}. Firstly, as the small nucleic acid drug, siTNF α shows rapid clearance and degradation *in vivo* and in drastic intracellular environment with large amounts of enzymes³⁰. Secondly, the macrophages in inflamed joints are hard to reach. Thirdly, the infiltrated siTNF α are still easy to efflux from joints due to the constantly movement^{28,29}. To solve these limitations, reprogrammed neutrophils which hold phagocytosis ability, rapid inflammation chemotaxis, and down-regulated pro-inflammatory ability, would be a perfect siTNF α vector for targeting macrophages.

Herein, we described a reprogrammed siTNF α /neutrophil cytopharmaceutical (siTNF α /TP/NEs) with down-regulated TNF α expression for RA treatment, which can both inhibit the TNF α production by macrophages in inflamed joints, and regulate the gene expression like a disintegrin and metalloproteinase with thrombospondin motifs 5 (ADAMTS5) and matrix metalloprotein (MMP)-13 to protect cartilage. To prepare the siTNF α /TP/NEs, dual-protected siTNF α lipoplexes (siTNF α /TP) were first fabricated using protamine to condense siRNA (prot/siTNF α), and followed by the encapsulation of tertiary amine-derived cationic liposomes with the ability of endo/lysosomal escape by repeated freezing and thawing. The obtained siTNF α /TP which could circumvent the degradation of siTNF α engulfed in neutrophils, acted as an editor to reprogram neutrophils *ex vivo* to obtain the siTNF α /neutrophil cytopharmaceuticals (siTNF α /TP/NEs). siTNF α /TP/NEs held the potential of reduced productions of TNF α , thereby bypassing the pro-inflammatory ability of neutrophils but remaining their inflammation chemotaxis capability. After intravenous injection into the mice with collagen-induced arthritis (CIA), siTNF α /TP/NEs could successfully arrive at the inflamed joints in response to the chemoattractants from inflamed joints, followed by the release of siTNF α /TP due to the formation of NETs, which is sequentially phagocytosed by macrophages to inhibit TNF α expression. Of note, the apoptotic siTNF α /TP/NEs could also be phagocytosed by macrophages which would convert to the anti-inflammatory phenotype due to the phagocytosis of apoptotic neutrophils³¹. We have demonstrated that the reprogrammed siRNA/neutrophil cytopharmaceuticals with down-regulated TNF α production can effectively deliver siTNF α to macrophages in inflamed joints and downregulate the TNF α expression, thus leading to the relieve of local inflammation and protection of cartilage (Fig. 1). The reprogrammed siRNA/neutrophil cytopharmaceuticals combine the merits of inflammation-targeting of neutrophils as well as the gene silencing of siTNF α , which provide a novel treatment paradigm for RA and put forward a vector platform of gene therapy for inflammation-associated diseases.

2. Materials and methods

2.1. Materials, cell lines, and animals

Scrambled siRNA (siNC) (sense strand: 5'-UucuccgaacgugucacgudTdT-3', anti-sense strand: 3'-AcgugacacguucggagaadTdT-5'), siTNF α (anti-sense strand: 5'-CgtcgtagcaaacaccacaaadTdT-3'), fluorescein-labeled scrambled siRNA (FAM-siRNA) and Cy5-labeled scrambled siRNA (Cy5-siRNA) were purchased from RiboBio (Guangzhou, China). Protamine sulfate (MW ~5000 Da) was purchased from Yuanyebio (Shanghai, China). RNA isolater total RNA extraction reagent and SYBR Green

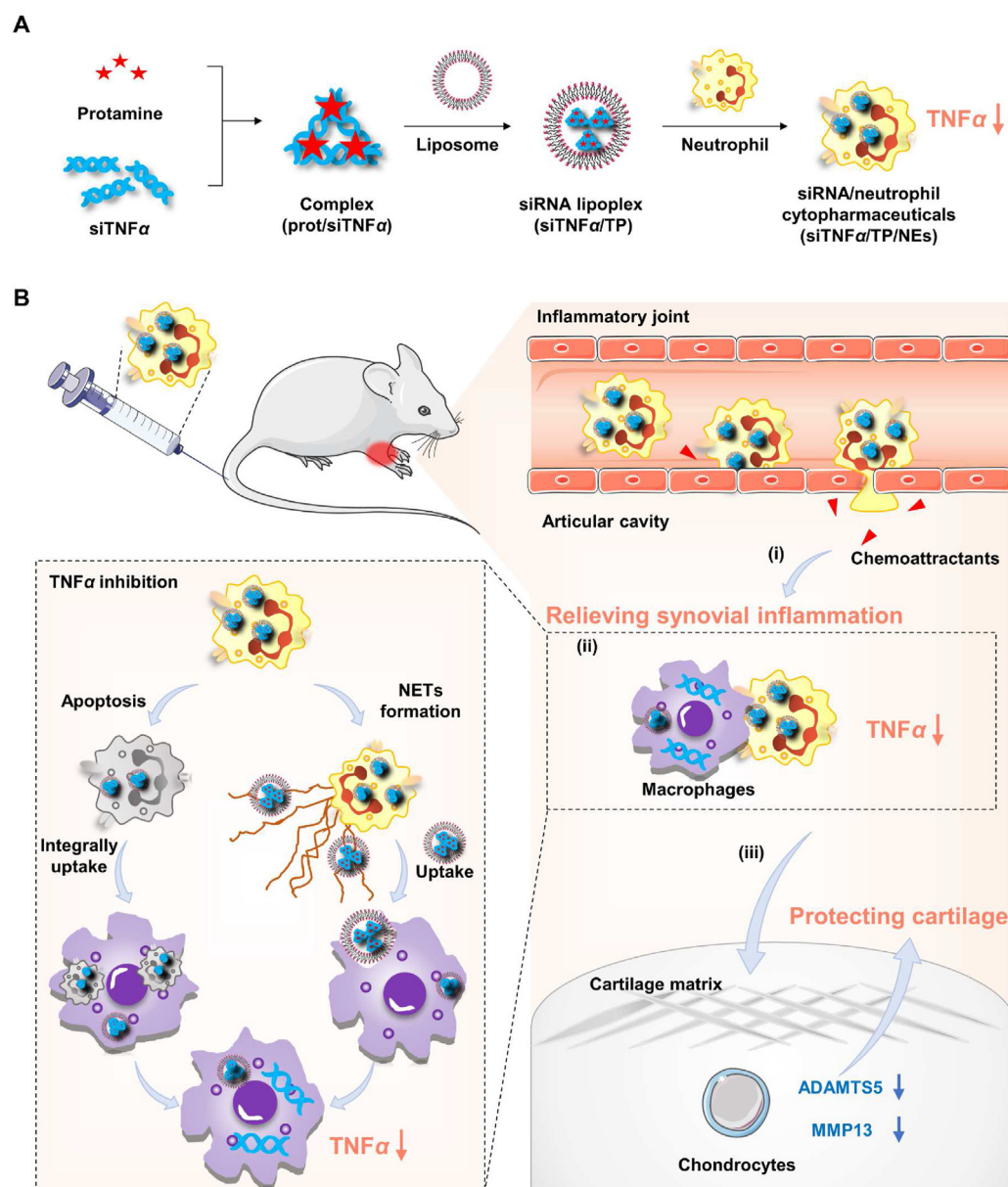


Figure 1 Schematic illustration of the reprogrammed siRNA/neutrophil cytopharmaceuticals for suppressing synovial inflammation and ameliorating joint destruction in inflammatory arthritis. (A) Preparation of the reprogrammed siRNA/neutrophil cytopharmaceuticals with down-regulated TNF α . siTNF α was first condensed with protamine to form a complex (prot/siTNF α), and then encapsulated by tertiary amine-derived cationic liposomes to gain a lipoplex (siTNF α /TP), followed by the uptake by neutrophils to obtain the reprogrammed siRNA/neutrophil cytopharmaceuticals (siTNF α /TP/NEs). (B) The *in vivo* mechanisms of siTNF α /TP/NEs against inflamed joints. (i) After intravenous injection into collagen-induced arthritis (CIA) mice, siTNF α /TP/NEs can migrate along a gradient of chemoattractants to the inflamed joints leveraging the chemotaxis of neutrophils. (ii) When arrive at the inflammatory joints, siTNF α /TP/NEs can release the encapsulated siTNF α /TP through the formation of NETs. Both the released siTNF α /TP and the apoptotic siTNF α /TP/NEs can be phagocytosed by macrophages, which effectively deliver the siTNF α to macrophages in inflamed joints, thus reducing the TNF α expression. (iii) The downregulation of TNF α level can modulate the inflammatory network and result in the relief of local inflammation and protection of cartilages.

Master Mix were purchased from Vazyme Biotech Co., Ltd. (Nanjing, China). 2-Dioleoyl-*sn*-glycero-3-phosphoethanolamine (DOPE) was obtained from AVT Pharmaceutical Technology (Shanghai, China). Rhodamine B 1,2-dihexadecanoyl-*sn*-glycero-3-phosphoethanolamine, triethylammonium salt (Rhodamine DHPE) was purchased from ThermoFisher Scientific Co., Ltd. (USA). Ditetradecyl (4-((2-(1-methylpyrrolidin-2-yl)ethyl) amino)-4-oxobutanoyl) glutamate (TA7) was prepared by our lab.

The RAW264.7 cells and mouse fibroblast (L929) cells were purchased from the Shanghai Cell Bank (Shanghai, China), and cultured in DMEM medium with 10% of foetal bovine serum (Gibco, USA) and 1% penicillin–streptomycin solution (Hyclone, USA). The incubate condition was maintained at 37 °C in a humidified 5% CO₂ atmosphere.

C57BL/6 mice (6–8 weeks, male) were purchased from the Zhejiang Academy of Medical Sciences. All the animals were

treated in accordance with the Guide for Care and Use of Laboratory Animals, approved by the Animal Experimentation Ethics Committee of China Pharmaceutical University.

2.2. Preparation of siTNF α /TP

Protamine (prot, at a final concentration of 1 mg/mL) was complexed with siTNF α (at a final concentration of 1 mg/mL) in free nuclease water at a 1.2/1 M ratio (prot/siRNA), mixed by vortex for few seconds and incubated at room temperature for 10 min³².

To obtain TA7 liposomes, TA7 and DOPE at a mass ratio of 1/1 were dissolved in a mixture of CHCl₃ and methanol (3/2, v/v), followed by evaporation to form a thin film. Then, 3 mL of deionized water was added to hydrate the film at 37 °C for 0.5 h. The cationic TA7 liposomes was obtained by sonication in a bath sonicator (Atpio, Nanjing, China) and filtration through a 0.45 μ m polycarbonate membrane. The particle sizes and zeta potentials of TA7 liposomes with the corresponding polydispersity index (PDI) were determined by dynamic light scattering (DLS) using a Zetasizer Nano ZS instrument (Malvern, UK). Similarly, rhodamine B-labeled liposomes (RHO-TA7) were prepared as the same procedure except for adding 0.4% (w/w) rhodamine-DHPE.

siTNF α /TP were obtained by trapping prot/siRNA into pre-formed TA7 liposomes as follows. Prot/siRNA polyplexes were incubated with TA7 liposomes for 8 min at room temperature, five freezing and thawing cycles were then performed. For each cycle, freezing was achieved in liquid nitrogen for 1 min and thawing in a water bath at 60 °C for 2 min. Afterwards, the particle sizes and zeta potentials of the polyplexes with different N/P ratios were detected. Meanwhile, agarose gel electrophoresis was performed to check the encapsulation of siRNA in different steps of the preparation. Samples were tested by agarose gel electrophoresis at 120 V for 15 min, followed by visualization at 312 nm using a gel visualizing system (Tanon, Tanon 3500, Shanghai, China). In addition, fluorescently labeled siTNF α /TP (FAM-siRNA/RHO-TP) were prepared similarly by substituting the siTNF α by FAM-siRNA and the TA7 liposomes by RHO-TA7 liposomes. While FAM-siRNA/RHO-TA7 were prepared by the direct mixture of FAM-siRNA and RHO-TA7 liposomes at the room temperature.

2.3. Isolation of murine NEs from bone marrow

Mature NEs were isolated from murine bone marrow using a modified method as reported^{33,34}. Briefly, the femurs and tibias of mice were isolated and immersed in RPMI 1640 medium (Hyclone) after removal of the muscle and sinew. Bone marrow was flushed from the bone with phosphate-buffered saline (PBS), followed by centrifugation at 200 \times g for 3 min (Cence, TG16WS, Hunan, China). The supernatant was removed carefully, and the pellet was re-dispersed into 3 mL of red blood cell lysis buffer. Then the resulted mixture was centrifuged (1000 rpm, 5 min). The obtained cell pellet was re-dispersed into 2 mL of RPMI 1640 medium to obtain the unicellular suspension, which was then added into a Percoll mixture solution consisting of 55%, 65% and 75% (v/v) Percoll in PBS, followed by centrifugation at 1000 \times g for 30 min. The mature NEs were recovered at the interface of the 65% and 55% fractions and washed by ice-cold PBS thrice. The purity was determined using immunofluorescence double staining with violent 421-conjugated Ly-6G antibody (BioLegend, CA, USA) and phycoerythrin (PE)-conjugated CD11b antibody (BioLegend), and detected by using flow cytometry (Invitrogen, CA, USA). The morphology of NEs stained with Wright-Giemsa

(Jiancheng, Nanjing, China) was observed by an optical microscope (Nikon, Ts2R, Japan).

2.4. Preparation and characterization of siTNF α /TP/NEs

Briefly, the obtained bone marrow neutrophils (1×10^6 cell/mL) were co-incubated with siTNF α /TP (siTNF α concentration: 100 nmol/L) in RPMI 1640 medium at 37 °C for 1 h. The mixture was then centrifuged (1000 rpm, 5 min) and washed thrice with PBS to get the siTNF α /TP/NEs. Similarly, dual-labeled neutrophil cytopharmaceuticals (FAM-siRNA/RHO-TP/NEs) were prepared using the same procedure except for using FAM-siRNA/RHO-TP. The cellular viability of prepared neutrophil cytopharmaceuticals was measured by Cell Counting Kit-8 (CCK-8, Beyotime, China) according to the manufacturer's instructions. After 8 h of incubation, absorbance (OD value) was detected by Synergy (Biotech, USA) at the wavelength of 450 nm.

To quantify the loading efficiency and encapsulation efficiency, Cy5-siRNA/TP/NEs were placed on a 96-well plate, and the fluorescence intensity of Cy5-siRNA/TP/NEs was analyzed by Synergy (Biotech) (excitation wavelength at 625 nm, emission wavelength at 670 nm). The loading efficiency (the amount of loading Cy5-siRNA/the numbers of neutrophils) and encapsulation efficiency (the amount of loading Cy5-siRNA/the feeding amount of Cy5-siRNA \times 100%) of siTNF α /TP/NEs were calculated following the standard curve of Cy5-siRNA.

The stability of siTNF α /TP/NEs was detected by confocal laser scanning microscopy (CLSM) (ZEISS, LSM 880, Germany). FAM-siRNA/RHO-TP/NEs were prepared and cultured in dark for different times (0, 1, 2, 4, 6, and 8 h), then 1 mL of Hoechst 33342 (v/v = 1/1000) was added to stain for 10 min. After that, FAM-siRNA/RHO-TP/NEs were observed and photographed under CLSM. At the same time, FAM-siRNA/RHO-TA7/NEs were prepared as controls. The final concentration of FAM-siRNA in each dish was 100 nmol/L.

To measure the migration capacity of neutrophils or neutrophil cyto-pharmaceuticals towards inflammation, a Transwell chamber with 3 μ m pore size (Millipore, MA, USA) was used. The chambers were placed on a 24-well plate with each well containing 0.8 mL of completed RPMI 1640 medium with 100 nmol/L N-formyl-L-methionyl-L-leucyl-L-phenylalanine (fMLP). Then 1×10^6 neutrophils or siTNF α /TP/NEs were placed into the upper chamber, respectively, which was then incubated at 37 °C for 3 h. At the end of incubation, the lower chamber was imaged by an optical microscope (Nikon) and the number of migrated cells was analyzed by Image J.

Relative migrated cells (%) = The average number of cells in the lower chamber/The total number of feeding cells \times 100 (1)

2.5. Evaluation of the anti-inflammatory effect of siTNF α /TP/NEs

To access the endo/lysosomal escape ability of siTNF α /TP in neutrophils, the FAM-siRNA/TP was incubated with neutrophils for 4 h 15 min before observation under CLSM, Lyso-Tracker Red was added to label the endo/lysosomes at a final concentration of 100 nmol/L. Then, Hoechst 33342 was added to gain a final concentration of 0.5 μ g/mL. After staining of 15 min against light, culture plates were washed three times with PBS, and images were captured as soon as possible with a CLSM. The method of endo/lysosomal escape ability of siTNF α /TP in macrophages was the same as above.

To determine the reprogramming effect of siTNF α /TP/NEs, the blank neutrophils, siNC/TP/NEs and siTNF α /TP/NEs were seeded in 24-well plates. Then, the cells were stimulated with lipopolysaccharide (LPS) (200 ng/mL) for 2 h. The culture mediums were collected to proceed enzyme linked immunosorbent assay (ELISA) analysis. After wash thrice with PBS, the cells were collected to proceed the quantitative real-time polymerase chain reaction (q-PCR).

For ELISA assay, TNF α levels in the supernatant were measured using mouse ELISA kits (Elabscience, Wuhan, China) as recommended by the manufacturer.

For q-PCR assay, total RNA was extracted from treated cells using RNA isolater total RNA extraction reagent according to standard protocol. 1000 ng of total RNA was transcribed into cDNA using HiScript II SuperMix (Vazyme, Nanjing, China) for q-PCR. 1 μ L of cDNA, 5 μ L of AceQ q-PCR SYBR Green Master Mix (High ROX Premixed), 3 μ L of DEPC water, 0.5 μ L of forward primer (10 μ mol/L) and 0.5 μ L of reverse primer (10 μ mol/L) for TNF α and β -actin were mixed and sampled by the q-PCR analysis (StepOne™ System, USA). The primers used in the q-PCR for *Tnf α* , *Mmp9*, *Tgf- β* , *Adamts5*, *Mmp13* and β -actin were 5'-GGGAGAGTGGTCAGGTTGCC-3' (*Tnf α* forward), 5'-TCAGGGAAGAATCTGGGAAAGGT-3' (*Tnf α* reverse), 5'-AAACCTC-CAACCTCACGGAC-3' (*Mmp9* forward), 5'-ACAACCTCGTCGTCGCGAAA-3' (*Mmp9* reverse), 5'-ACTGGAGTTGTACGGCAGT G-3' (*Tgf- β* forward), 5'-GGGGCTGATCCCGTTGATTT-3' (*Tgf- β* reverse), 5'-GCAGGGAACATAGGCAGGTT-3' (*Adamts5* forward), 5'-ACCAAATATTCGGTTAGGCTGA-3' (*Adamts5* reverse), 5'-ACCCAGCCCTATCCCTTGAT-3' (*Mmp13* forward), 5'-TC TTCCATGTGGTTCCAGCC-3' (*Mmp13* reverse), 5'-CCAACCG CGAGAAGATGA-3' (β -actin forward) and 5'-CCAGAGGCGTA-CAGGGATAG-3' (β -actin reverse), respectively.

2.6. Isolation of bone marrow-derived macrophages

Bone marrow cells were isolated from the femurs of mice. Cells were seeded in dishes (15 cm) in DMEM medium containing 30% of L929 cell-conditioned medium and 10% of FBS. After 3 days, the cells received fresh supplemented medium in the same proportion and were incubated for another 5 days. Then, the cell medium was replaced by fresh medium in the same proportion. And cells were incubated till another 7 days to be mature.

2.7. Transfer of siTNF α /TP from neutrophils to macrophages

To further visualize the release of siRNA from neutrophil cytopharmaceuticals and uptake by macrophages. FAM-siRNA/RHO-TP/NEs were incubated in DMEM with IL1 β (10 ng/mL). At 0, 0.5, 2, 4, 6, and 8 h, the cells were fixed with 4% paraformaldehyde for 30 min and blocked with 5% Bovine Serum Albumin (Solarbio, Beijing, China) for 1 h, then incubated with anti-citrullinated Histone H3 (Abcam, ab5103, 1:1000 dilution) at 4 °C overnight. Alexa Flour 633-labelled goat anti-rabbit secondary antibody (Invitrogen, A21071, 1:1000 dilution) was applied to label citrullinated Histone H3. CLSM was used to observe the formation of NETs as well as the released FAM-siRNA/RHO-TP.

To further determine the uptake of siTNF α /TP by macrophages, BMDM and RAW 264.7 cells were incubated with Cy5-siRNA/TP/NEs for 8 h with IL1 β (10 ng/mL) for stimulation. Neutrophils were labeled by FITC-Ly6G. Then, CLSM was used to observe the phagocytosis of macrophages over time.

2.8. In vitro gene silencing efficiency

To evaluate the *in vitro* gene silencing efficiency of siTNF α /TP/NEs, RAW264.7 cells or BMDM cells were seeded in 24-well plates and cultured with DMEM medium with 10% of FBS and 1% penicillin-streptomycin solution for 24 h. Then, the cells were cultured in the FBS-free DMEM medium and incubated with blank NEs, siNC/TP/NEs, siTNF α /TP and blank NEs, as well as siTNF α /TP/NEs (100 nmol/L of siTNF α) for 6 h, respectively. Then, the medium was replaced by fresh culture medium containing 10% of FBS and cultured with LPS (200 ng/mL) for another 2 h. After that, the cells and the culture medium were collected for q-PCR and ELISA analysis as described above.

2.9. CIA mice model construction

The CIA mice were established by a double immunization strategy. For the first immunization, mice were injected intradermally at the end of the tail with an emulsion of equal volume chicken type-II collagen solution (2 mg/mL) and complete Freund's adjuvant (5 mg/mL). After 21 days of the first immunization, the boost immunization was given to the mice with chicken type-II collagen solution (2 mg/mL) emulsified in incomplete Freund's adjuvant (5 mg/mL).

2.10. Biodistribution of neutrophil cytopharmaceuticals

The CIA mice were intravenously injected with different formulations including Cy5-siRNA, Cy5-siRNA/TP and Cy5-siRNA/TP/NEs. Each group ($n = 3$) were administrated with Cy5-siRNA at a dose of 0.3 mg/kg. At different time post-injection, the images were acquired using IVIS® Spectrum Imaging System (PerkinElmer, MA, USA). At 24 h post-injection, all the mice were sacrificed. The legs and normal tissues were harvested for *ex vivo* imaging. The joints were collected for frozen section. The slices were stained with FITC-F4/80 (Biolegend) overnight at 4 °C. CLSM was used to observe the distribution of Cy5-siRNA in synovium.

2.11. In vivo therapeutic efficacy of siTNF α /TP/NEs in CIA mice

To study the therapeutic efficacy, 200 μ L of saline, siTNF α /TP (0.3 mg/mL), siNC/TP/NEs (0.3 mg/mL), MTX (0.75 mg/kg), siTNF α /TP/NEs (0.3 mg/mL) were intravenously administrated into CIA mice since days 24 at every three days (totally eight injections). MTX was used as a positive control and saline as a negative control.

Hind limbs of treated CIA mice were scored for severity of arthritis. The arthritis scores were evaluated using a scale of 0–4 for each paw. 0: normal paw with no erythema or swelling; 1: mild swelling and erythema restrict to the tarsals or ankle joint; 2: mild swelling and erythema extending from the ankle to the tarsus; 3: moderate swelling and erythema extending from the ankle to metatarsal joints; and 4: severe swelling and erythema involving the ankle, feet, and digits, or ankylosis of the limbs. Hind paw thickness was measured with an electric caliper placed across the ankle joint at the widest point. In addition, we collected blood from mice in each group at every week after the primary immunization, and serum TNF α levels were determined by ELISA assay. After euthanasia, knee joints tissues from CIA mice ($n = 3$ per each group) were ground in liquid nitrogen and

total RNA was extracted for detecting the joint *Tnfα* mRNA by q-PCR.

At the endpoint of the study, mice from each group were used for MRI scanning, respectively ($n = 3$, at each group). MRI studies were performed using a Bruker pharmscan 7.0T scanner (Bruker Biospin, Ettlingen, Germany) with 38 mm coil. Briefly, mice were anesthetized in 2% inhaled isoflurane in oxygen and then positioned on an imaging platform for localization scanning. The respiratory rate needed to maintain of 30–80 breaths/min. The scanning sequence included short time inversion recovery and T2 mapping scanning. The acquisition parameters were as follows: repetition time (TR) = 2500 ms³⁵.

In addition, the joints tissues of each group were collected and fixed in 4% paraformaldehyde for at least 72 h. Then the fixed tissues were decalcified in EDTA buffer (20% EDTA, pH 7.4) for at least 7 days. Subsequently, tissues were embedded in paraffin. Serial sections (4 μm) were stained with hematoxylin & eosin (H&E) and safranin O-fast green. For histological analysis, paraffin sections stained with H&E or safranin O-fast green were visualized by the optical microscope (Leica, DM5500B, Germany). For immunohistochemistry, the paraffin-embedded sections were stained with rabbit anti-TNFα, anti-ADAMTS5, or anti-MMP13 (Abcam, USA), respectively, followed by stained with the DAB chromogen kit (Servicebio, Wuhan, China). The mean optical density value was acquired using Image-Pro Plus 6.0 software (Media Cybernetic) by dividing the sum of the optical density of each pixel in the area by the area sizes.

Moreover, the fixed knee joints of CIA mice were scanned using micro-CT (Bruker, SkyScan 1176, Germany). The scanner was set at a resolution of 18 μm with 70 kV of voltage and 114 μA of electric current. We defined the region of interest (ROI) to cover the whole subchondral bone in tibial plateaus. The three-dimensional reconstruction was conducted by Mimics 17.0 software (Materialise).

2.12. Statistical analysis

The results are presented as means ± standard error of the mean (means ± SEM) as indicated. The data were compared by Student's *t*-test between two groups and ordinary one-way analysis of variance (ANOVA) for three or more groups. All statistical analyses were conducted by the GraphPad Prism software. The threshold of a statistically significant difference was defined as * $P < 0.05$, ** $P < 0.01$, *** $P < 0.001$, **** $P < 0.0001$, and ns as no significance. The significance of pairwise group is shown on the top of the corresponding line. No significance, ns; * $P < 0.05$; ** $P < 0.01$; *** $P < 0.001$; **** $P < 0.0001$.

3. Results

3.1. Preparation and characterization of siRNA/neutrophil cytopharmaceuticals (siTNFα/TP/NEs)

For proof of our idea, we first prepared the siRNA lipoplex (siTNFα/TP) through two steps to improve its stability in neutrophils (Fig. 2A). Firstly, protamine, a typically positive protein (about 50–110 amino acids)³⁶, was used to condense siTNFα to gain a prot/siTNFα complex. To investigate the optimal weight ratio of prot/siTNFα, we performed agarose gel electrophoresis to confirm that siTNFα could be completely condensed by protamine. We found that no siRNA leaked at the weight ratio (w/w) of

1.2 and 1.6 of prot/siTNFα (Supporting Information Fig. S1A). Moreover, the particle sizes of prot/siTNFα at the weight ratio (w/w) of 1.2 and 1.6 were stable, both of which possessed a positive charge (Fig. S1B). To gain the balance between stable encapsulation and efficient release of siRNA, the weight ratio (w/w) of prot/siTNFα at 1.2 was identified as the optimum. The obtained prot/siTNFα showed a particle size of 347.53 nm and a positive charge of +9.28 mV (Supporting Information Table S1), which seemed like unregular complex by TEM images (Fig. 2A).

Then, we fabricated cationic liposomes composed of tertiary amine-derived cationic lipid (TA7) and DOPE at an optimal mole ratio of 1/1 according to our previous report (Fig. 2A)³⁷. TA7 liposomes had demonstrated to be a safe and effective vector for siRNA delivery with superior endo/lysosomal escape ability, whose particle size and zeta potential were about 68.64 nm and +31.47 mV, respectively (Table S1). Thus, we encapsulated the prot/siTNFα by TA7 liposomes using five repeated freeze/thaw cycles to obtain the siTNFα/TP. To ensure the steady loading of siTNFα in TA7 liposomes, we optimized the N/P ratio (referring to the number of nitrogen residues (N) in the TA7 lipid to phosphate (P) of siTNFα) using agarose gel electrophoresis. When the N/P ratio is higher than 3, no siRNA band could be found (Supporting Information Fig. S2A). Moreover, the particle size and zeta potential of siTNFα/TP plateaued at the N/P ratio of 4 (Fig. S2B). Considering the above results, we chose N/P ratio of four for the fabrication of siTNFα/TP, which showed an average particle size of 180.93 nm and a positive charge of +29.71 mV (Table S1). Owing to the encapsulation of prot/siTNFα, the particle size of siTNFα/TP increased about 100 nm than that of TA7 liposomes. While the surface charge of siTNFα/TP were comparable to TA7 liposomes, indicating the encapsulation of prot/siTNFα within liposomes. To further verify whether siTNFα is inside of TA7 liposomes, agarose gel electrophoresis and transmission electron microscopy (TEM) were applied. If siTNFα were outside of liposomes, they would be replaced by heparin with negatively charge, and the free siRNA band could be observed. However, we did not find the free band of siTNFα after the incubation of siTNFα/TP and heparin, while the control group of siTNFα/TA7 which fabricated by the simple complex of TA7 liposomes and siTNFα displayed obvious siRNA band (Supporting Information Fig. S3). In addition, the TEM image of siTNFα/TP showed a uniformly smooth spherical structure with obvious core-shell structure (Fig. 2A), which was different from that of prot/siTNFα and TA7 liposomes. These results indicated that prot/siTNFα had been encapsulated inside TA7 liposomes, which would further improve the stability of siTNFα in neutrophils.

Next, we isolated neutrophils from mouse bone marrow^{33,34,38,39}, and purified by density gradient centrifugation. The isolated neutrophils showed a purity of 93% labeled by dual-positive of CD11b and Ly6G, the typical biomarkers of neutrophils (Fig. 2B), and held the typical lobular shape of the neutrophil nuclei stained by Giemsa-Wright (Fig. 2C). The purified neutrophils were incubated with siTNFα/TP at the optimal siTNFα concentration of 100 nmol/L and incubation time of 1 h to obtain siTNFα/TP/NEs (Fig. 2D). We found that when the concentration of siTNFα/TP was lower than 100 nmol/L, the viability of neutrophils was higher than 80% (Supporting Information Fig. S4). And the incubation time of 1 h obtained the plateaued amount of siTNFα within neutrophils (Supporting Information Fig. S5). Moreover, CLSM was applied to validate the successful construction of siTNFα/TP/NEs by the fluorescence co-localization of Rhodamine B-labeled TA7 liposomes (RHO-TA7) and FAM-siRNA, which were distributed at the

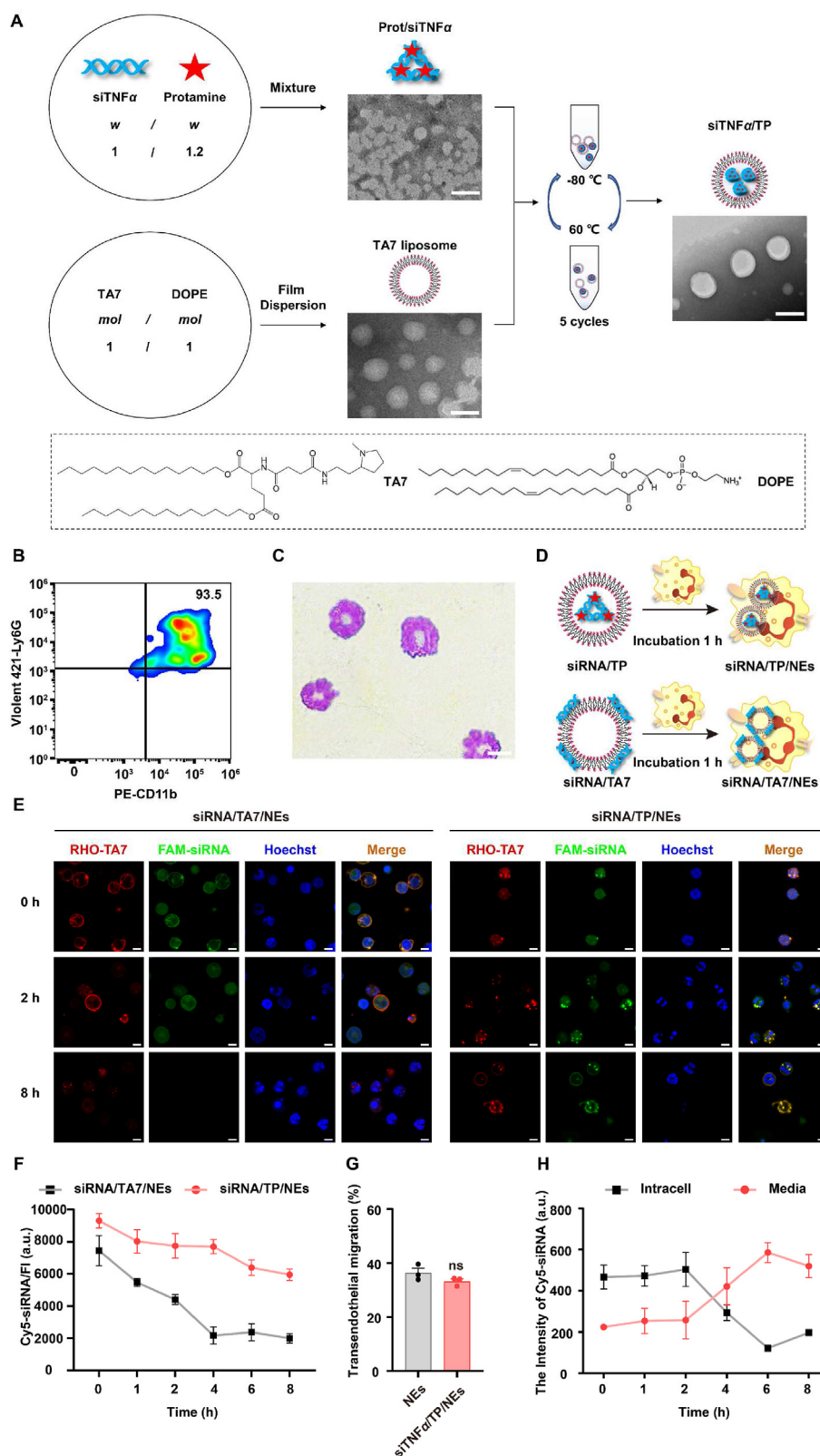


Figure 2 Preparation and characterization of siRNA/neutrophil cytopharmaceuticals (siTNF α /TP/NEs). (A) Schematic of the preparation of siTNF α /TP and the associate TEM images of prot/siTNF α , blank TA7 liposomes and siTNF α /TP, respectively. Scale bar: 100 nm. (B) Flow cytometry analysis of the purity of isolated neutrophils. Isolated neutrophils were double stained with PE anti-mouse CD11b and violenr-421 anti-mouse Ly6G antibodies. (C) Morphological images of isolated neutrophils stained with Giemsa–Wright stain. Scale bar: 5 μ m. (D) Schematic of the preparation of siRNA/TP/NEs and siRNA/TA7/NEs. (E) CLSM images of siRNA/TP/NEs after culturing at 37 $^{\circ}$ C for 8 h. The nuclei of neutrophils were stained with Hoechst 33342 (Blue), TA7 liposomes were stained with rhodamine B (Red), and siRNA was labeled with FAM

cytoplasm of neutrophils (Supporting Information Fig. S6). Additionally, we determined that the loading capacity of siRNA/neutrophil cytopharmaceuticals was about 0.03 nmol siRNA per million cells and the encapsulation efficiency was around 30%.

We further explored the intracellular stability of siTNF α /TP within neutrophils. For obviously monitoring, FAM-siRNA and Cy5-siRNA were used as models for CLSM and fluorescence detection, respectively. It was interesting to note that FAM-siRNA/TP maintained as a stable lipoplex observed by colocalization of green FAM-siRNA and red RHO-TA7 fluorescence within neutrophils for at least 8 h, whereas the simple complex of FAM-siRNA/TA7 rapidly disassembled less than 2 h due to the harsh intracellular microenvironment of neutrophils (Fig. 2D and E, Supporting Information Fig. S7). And at 8 h, the fluorescent intensity of Cy5-siRNA in siRNA/TP/NEs was as three times as that of siRNA/TA7/NEs (Fig. 2F), indicating the superiority of dual protection of siRNA through precondensation by protamine and the location inside TA7 liposomes. The improved stability of siRNA/TP within neutrophils provides a potential for the enhanced gene silence effect in macrophages.

Additionally, the inflammatory chemotaxis of siTNF α /TP/NEs determined the targeting ability to macrophages in inflamed joint. Thus, the migratory function of siTNF α /TP/NEs was tested *in vitro* using a Transwell migration assay, in which human umbilical vein endothelial cells (HUVEC) were laid in the porous membrane to mimic the vascular wall and fMLP as the chemoattractant of neutrophils was added into the lower chamber. The result shows that both siTNF α /TP/NEs and fresh neutrophils could respond to the inflammatory signals and migrate across the HUVEC layer without significant difference (Fig. 2G), which indicated that the loading process of siTNF α /TP had no effect on the motion and chemotaxis of neutrophils, implying the *in vivo* targeting potential of siTNF α /TP/NEs from injection site to the inflamed site. Lastly, the release kinetics of siRNA from neutrophil cytopharmaceuticals in inflammatory environment mimicked by phorbol myristate acetate (PMA) was detected. We found that the cytopharmaceuticals quickly released the loaded siRNA after 2 h incubation with PMA (Fig. 2H), suggesting the release ability of neutrophil cytopharmaceuticals in inflammatory environment. Overall, the prepared siRNA/neutrophil cytopharmaceuticals maintain the chemotaxis and inflammation responsibility of neutrophils, suggesting the favorability for the RA joints targeted gene delivery.

3.2. siTNF α /TP reprogrammed neutrophils against RA

To figure out whether siRNA can escape from the endo/lysosomes of the neutrophils to perform reprogramming, the intracellular transport of siRNA delivered by FAM-siRNA/TP was monitored by CLSM (Fig. 3A). After 0.5 h of incubation, most of FAM-siRNA (green) were colocalized with endo/lysosomes (red) as shown in a bright yellow fluorescence, while as time lapses, the green fluorescence gradually separated from the red fluorescence with the misalignment gray values. It suggested that most of siRNA could successfully escape from the endo/lysosomes into

the cytoplasm after 4 h, which provides a feasibility for the neutrophil reprogramming.

The outbreak of inflammation and cartilage injury caused by neutrophils might aggravate RA. We wondered whether the siTNF α /TP could reprogram neutrophils to anti-RA with efficacies from two aspects: the inflammation reduction by TNF α inhibition and the cartilage protection. To proof the successful inhibition of TNF α by siTNF α /TP, the *Tnf α* mRNA level in neutrophils was assessed by q-PCR at first. As shown in Fig. 3B, the mRNA level of *Tnf α* in siTNF α /TP/NEs stimulated by LPS significantly decreased over time, and about 50% decrease of *Tnf α* level in siTNF α /TP/NEs was found after culture for 9 h, while siNC/TP/NEs prepared by the same procedure except for the replacement of the functional siTNF α by scrambled siRNA (siNC) showed significant high *Tnf α* level. The amount of TNF α protein released by neutrophils was also detected by ELISA assay. Similar with the *Tnf α* mRNA level, siTNF α /TP/NEs stimulated by LPS exhibited about 59% reduction of TNF α production than siNC/TP/NEs (Supporting Information Fig. S8), demonstrating the effective inhibition of TNF α produced by neutrophils. In addition, due to the anti-inflammatory activity of neutrophils partly *via* the induction of transforming growth factor- β (*Tgf- β*), we further examined the level of *Tgf- β* mRNA in siTNF α /TP/NEs under LPS stimulation. The q-PCR results showed that compared to siNC/TP/NEs after LPS activation, siTNF α /TP/NEs increased the *Tgf- β* mRNA level to about 2.3-fold, mediating better anti-inflammatory property than unprogrammed neutrophils (Fig. 3C).

Besides, the limitation of neutrophils in RA treatment includes the matrix degradation through the secretion of MMP9⁴⁰, thus leading to the cartilage degradation. Here, we also examined the *Mmp9* level of siTNF α /TP/NEs to explore the protection of chondrocytes by reprogrammed neutrophils. Compared to LPS-activated-neutrophils and siNC/TP/NEs, LPS-activated siTNF α /TP/NEs significantly down-regulated the level of *Mmp9* mRNA (Fig. 3D), indicating that the decreased *Mmp9* level of reprogrammed neutrophils would be beneficial for the cartilage protection. Notably, chondrocytes in RA could either release the enzymes like ADAMTS5 and MMP13 to destroy the cartilage, which was highly related to the TNF α level in the environment. To further explore the improved protection of reprogrammed neutrophils with down-regulated TNF α expression on RA chondrocytes, siTNF α /TP/NEs were co-cultured with chondrocytes stimulated by IL1 β to mimic RA environment for determination of the levels of *Adamts5* and *Mmp13* in chondrocytes (Fig. 3E). After co-incubation with siTNF α /TP/NEs, the mRNA levels of *Adamts5* and *Mmp13* of chondrocytes both decreased obviously, suggesting the improved protection on cartilage (Fig. 3F and G). In contrast, the mRNA levels of *Adamts5* and *Mmp13* significantly upregulated after treatment with neutrophils or siNC/TP/NEs, indicating the cartilage destruction in RA by unprogrammed neutrophils. Moreover, when neutrophils and siTNF α /TP were co-incubated with chondrocytes, similar decreases of the *Adamts5* and *Mmp13* levels could be found, which suggested that the siTNF α /TP could be engulfed by neutrophils quickly and successfully reprogrammed the neutrophils to inhibit enzymes that associated with cartilage degradation in an inflammatory environment.

(Green). The merged image is the overlay of the three individual images. Scale bar: 5 μ m. (F) The fluorescent intensity of Cy5-siRNA in the siRNA/TP/NEs at different time, $n = 3$. (G) Percentage of migrated neutrophils in the lower chamber. Fresh neutrophils (NEs) were used as control. Data were presented as mean \pm SEM and analyzed by Student's *t*-test, $n = 3$. ns, not significant. (H) The release profile of Cy5-siRNA from siRNA/TP/NEs in RPMI 1640 medium with 100 nmol/L PMA ($n = 3$ per group).

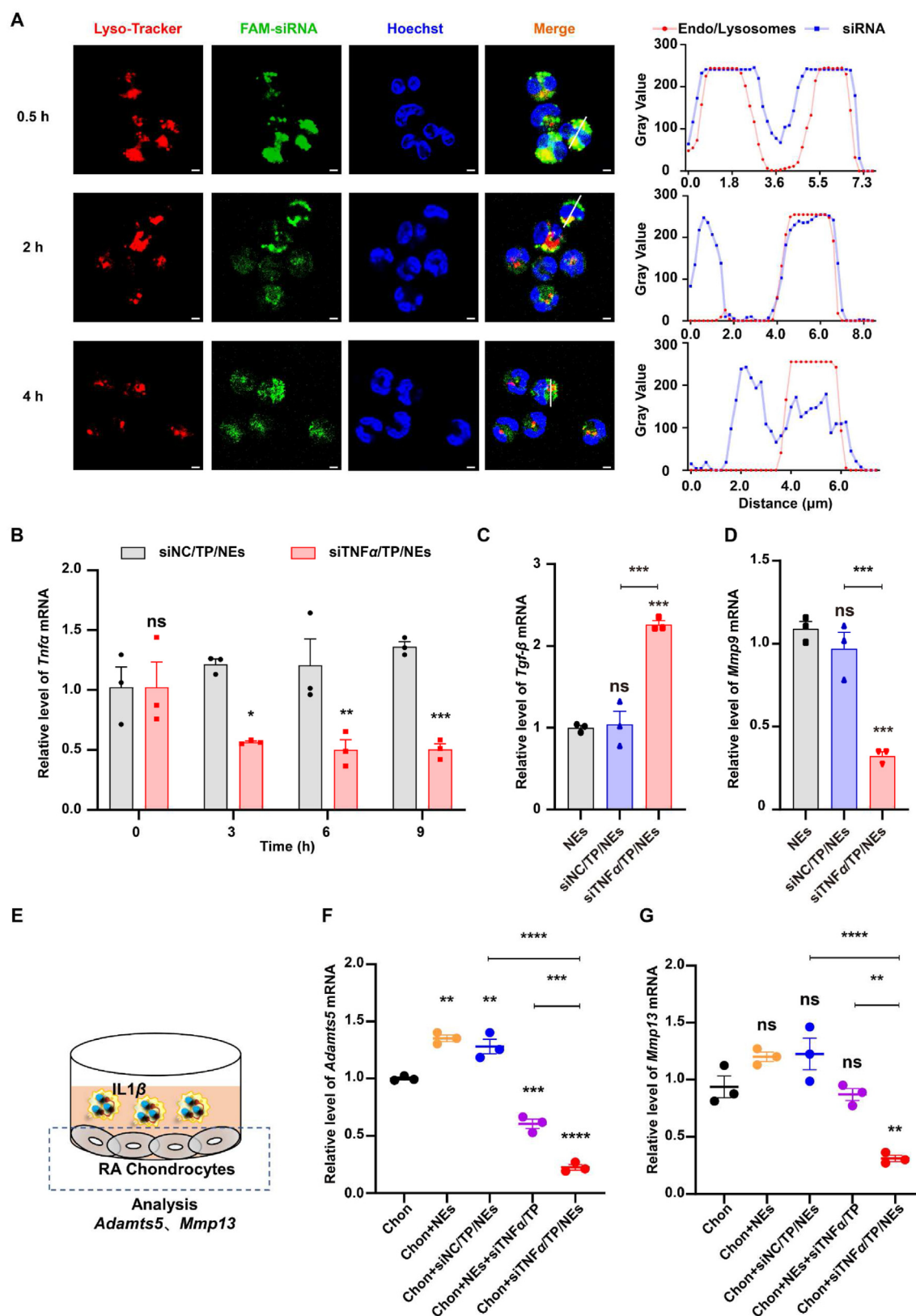


Figure 3 Reprogrammed neutrophils (siTNF α /TP/NEs) with anti-inflammatory ability and cartilage protection. (A) Time-dependent endo/lysosomal escape of siTNF α /TP in neutrophils. The representative gray values of endosomes and siRNA following the white line were analyzed by image J. Endo/lysosomes were stained with Lyso-Tracker Red, siRNA was labeled with FAM, and the nuclei were stained with Hoechst 33342. Scale bar: 2 μ m. (B) q-PCR assay of *Tnf α* mRNA in siTNF α /TP/NEs and siNC/TP/NEs with LPS stimulation. Data are presented as mean \pm SEM and analyzed by two-way ANOVA test with Sidak's correction, $n = 3$. siNC/TP/NEs set as control. ns, not significant, * $P < 0.05$, ** $P < 0.01$,

Taken together, we have successfully reprogrammed neutrophils through the engulfing the siTNF α /TP, which exhibited down-regulated *Tnf α* and *Mmp9* expressions, as well as up-regulated anti-inflammatory *Tgf- β* expression. Moreover, the reprogrammed neutrophils could inhibit the production of *Adams5* and *Mmp13* by RA chondrocytes, which further improved the potential of cartilage protection.

3.3. Transfer of siTNF α /TP to macrophages and the effective gene silencing of macrophages under inflammatory environment

The successful transfer of encapsulated siTNF α /TP to macrophages determines the gene silencing effect of TNF α in macrophages. We had demonstrated that siTNF α /TP could be released from siTNF α /TP/NEs in response to PMA. For further understand the mechanisms of siTNF α /TP release in RA environment, 10 ng/mL of IL1 β was used to mimic the RA environment. After 0.5 h incubation of IL1 β , siTNF α /TP/NEs showed an obvious formation of NETs which indicated by the typical markers-citrullinated histone H3 (CitH3) and chromatin stained by Hoechst 33342, and till 8 h, the formed NETs still existed (Fig. 4A, Supporting Information Fig. S9). Moreover, the colocalized FAM-siRNA and RHO-TA7 liposomes suggested the integrity of siTNF α /TP after the release from siTNF α /TP/NEs (Fig. 4A, Fig. S9). These results confirm the successful release of siTNF α from programmed neutrophils through the formation of NETs, and the intact siRNA lipoplex would aid the endocytosis of siRNA by macrophages.

To further confirm the uptake of by macrophages, siTNF α /TP/NEs were co-cultured with bone marrow-derived macrophages (BMDM) or RAW264.7 cells in the presence of IL1 β , respectively (Fig. 4B). We found that the signal of Cy5-siRNA gradually located within macrophages as the incubation time prolonged, indicating the successfully transfer of siRNA to macrophages. Interestingly, we found that Ly6G-labeled neutrophils loading with siRNA were also phagocyted by BMDMs (white arrowheads), it is suggested an alternative transfer approach of siRNA, which was similar with previous reports that macrophages could phagocyte the apoptotic neutrophils completely^{31,41,42}. Furthermore, phagocytosis of apoptotic neutrophils might lead to the phenotypic polarization of macrophages from pro-inflammatory type to anti-inflammatory one³¹, which would make for RA treatment.

Next, we assessed the endo/lysosomal escape ability of the siTNF α /TP in macrophages. As shown in Supporting Information Fig. S10, there is a colocalization (shown as yellow) of FAM-siRNA (green) and endo/lysosomes (red) after 0.5 h of incubation, demonstrating the effective siRNA/TP uptake by macrophages. Subsequently, siRNA/TP was able to escape from endo/lysosomes in a time-dependent fashion confirmed by the gradual differentiation between green and red signals. These results

validated that siRNA/TP also possessed the endo/lysosomal escape ability in macrophages, which would benefit for TNF α silencing.

To further investigate whether the transferred siTNF α remained fully bioactive after endo/lysosomal escape, the expression of TNF α in inflammatory macrophages (BMDM and RAW 264.7) was detected after treatment with reprogrammed siRNA/neutrophil cytopharmaceuticals. We first optimized the dosage that 1×10^6 siTNF α /TP/NEs treated with per 2×10^5 macrophages to make sure the significant inhibition of TNF α production by inflammatory macrophages after siTNF α /TP/NEs treatment (Supporting Information Fig. S11). Next, we compared the gene silencing efficiency of TNF α in macrophages treated with different formulations (Fig. 4C–F). q-PCR analysis showed that siTNF α /TP/NEs exhibited the strongest inhibition of about 68% and 70% on *Tnf α* mRNA in BMDM and RAW 264.7 cells, respectively, while the neutrophils alone and siNC/TP/NEs treatment showed an inflammation aggravation (Fig. 4C and E). It indicated that siTNF α /TP/NEs could significantly downregulate the TNF α expression by macrophages and even counteract the upregulation of TNF α expression induced by neutrophils. Similarly, the ELISA assays showed that macrophages treated with siTNF α /TP/NEs exhibited a 36% and 20% decrease of TNF α secretion in BMDM and RAW264.7 cells, respectively (Fig. 4D and F). In contrast, neutrophils alone or siNC/TP/NEs could improve the TNF α production in inflammatory environment, implying the significance of neutrophil reprogramming.

Collectively, reprogrammed neutrophil cytopharmaceuticals hold the merits of successful transfer of siTNF α to macrophages through release by NETs formation or integral uptake by macrophages, and the following potent TNF α gene silencing effect, which could be potential in RA treatment.

3.4. Biodistribution of siTNF α /TP/NEs

To assess the endogenous inflammation-targeting ability of reprogrammed siRNA/neutrophil cytopharmaceuticals *in vivo*, Cy5-siRNA were used as a near-infrared fluorescent siRNA for *in vivo* biodistribution. And collagen induced arthritis (CIA) mice were fabricated by the common two-step immunization approach, with severely red and swollen joints (Supporting Information Fig. S12). Free Cy5-siRNA, Cy5-siRNA/TP, and Cy5-siRNA/TP/NEs were injected intravenously into CIA mice at an identical Cy5-siRNA dose of 0.3 mg/kg, respectively. As shown in Fig. 5A and Supporting Information Fig. S13, Cy5-siRNA/TP/NEs emitted strongest fluorescence in paws at 2 h post-injection, compared to that of free Cy5-siRNA and Cy5-siRNA/TP, indicating the improved *in vivo* targeting ability of siRNA/TP/NEs to inflamed joints, which probably due to the naive chemotaxis of neutrophils. Moreover, the retention time of siRNA delivered by neutrophils obviously increased to even 24 h, whereas free Cy5-

*** $P < 0.001$. (C–D) q-PCR assays of (C) *Tgf- β* and (D) *Mmp9* mRNA in neutrophils (NEs in the figure), siNC/TP/NEs and siTNF α /TP/NEs stimulated by LPS, respectively. Data are presented as mean \pm SEM and analyzed by one-way ANOVA test with Turkey's correction, $n = 3$. NEs group was used as a control. ns, not significant, *** $P < 0.001$. The significance of pairwise group is shown on the top of the corresponding line. ### $P < 0.001$. (E) Schematic illustration of the *in vitro* model to evaluate the effect of siTNF α /TP/NEs on chondrocytes stimulated by IL1 β to mimic the RA environment. (F–G) q-PCR assays of (F) *Adams5* and (G) *Mmp13* mRNA in chondrocytes (Chon) stimulated by IL-1 β . Data are presented as mean \pm SEM and analyzed by one-way ANOVA test with Turkey's correction, $n = 3$. Chon group was used as a control. ns, not significant, ** $P < 0.01$; *** $P < 0.001$, **** $P < 0.0001$. The significance of pairwise group is shown on the top of the corresponding line. ## $P < 0.01$, ### $P < 0.001$, #### $P < 0.0001$.

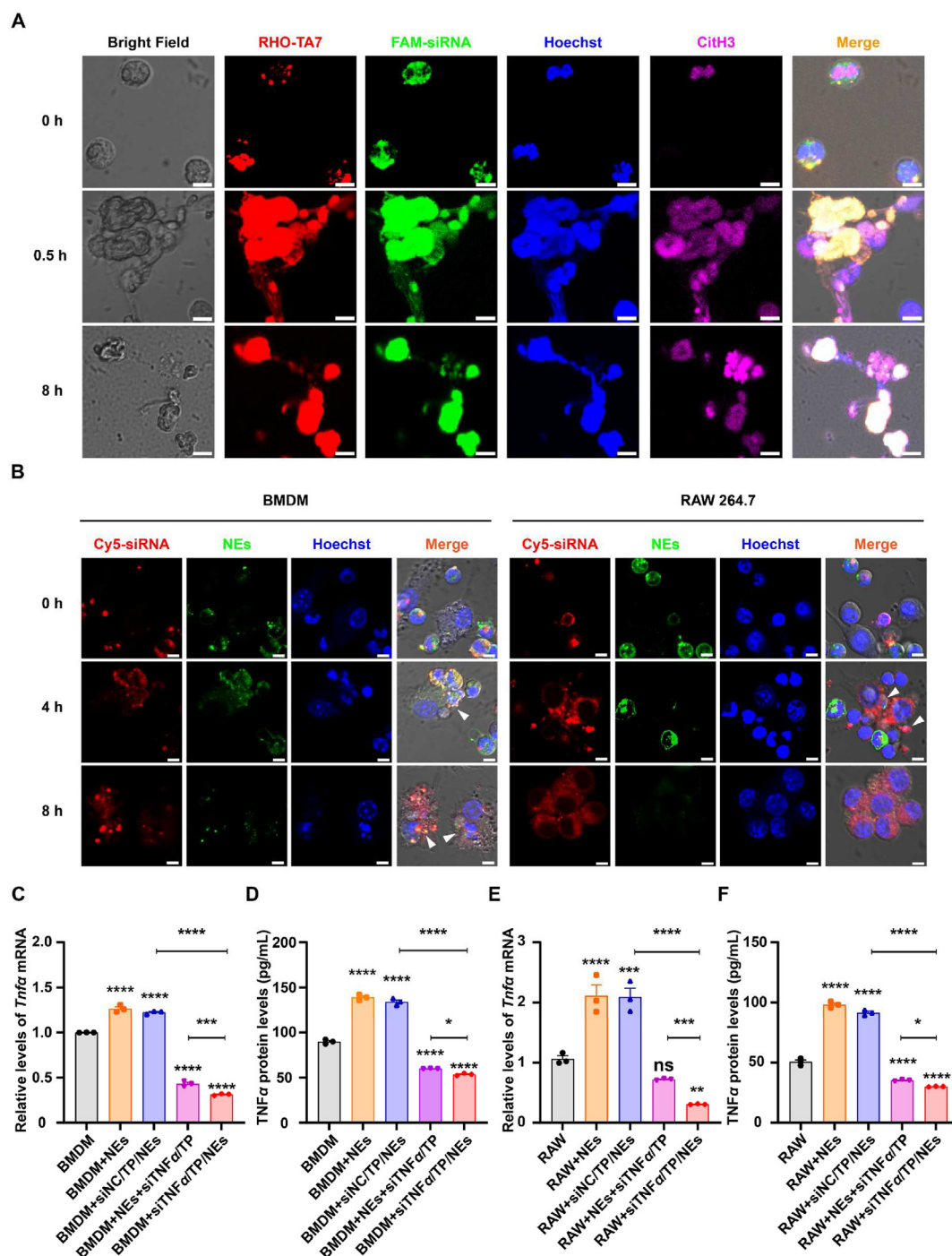


Figure 4 The transfer of siTNF α to macrophages including BMDM and RAW264.7 cells under inflammatory conditions and the following TNF α gene silencing. (A) CLSM images of siTNF α /TP released from siTNF α /TP/NEs through NETs formation in mimic RA environment with IL-1 β (10 ng/mL). siTNF α /TP/NEs were stained with Hoechst 33342 (Blue) and citrullinated Histone H3 (Violet), which were the typical markers of NETs. TA7 liposomes were labeled with rhodamine B (RHO-TA7, Red), and siRNA was labeled with FAM (FAM-siRNA, Green). Scale bars: 5 μ m. (B) CLSM images of BMDM and RAW264.7 cells after incubation with siTNF α /TP/NEs for 8 h siRNA was labeled with Cy5 (Cy5-siRNA, Red), neutrophils were stained by fluorescein isothiocyanate (FITC)-conjugated Ly6G (NEs, green). Arrowheads indicate the process of macrophages engulfing neutrophils. Scale bars: 5 μ m. (C–F) Measurement of TNF α expression in (C, D) BMDM and (E, F) RAW264.7 cells after LPS (200 ng/mL) stimulation and quantification by q-PCR and ELISA, respectively. Data were presented as mean \pm SEM and analyzed by one-way ANOVA test with Turkey's correction, $n = 3$. BMDM or RAW group was used as a control, respectively. ns, not significant, ** $P < 0.01$, *** $P < 0.001$, **** $P < 0.0001$. The significance of pairwise group is shown on the top of the corresponding line. * $P < 0.05$, ### $P < 0.001$, #### $P < 0.0001$.

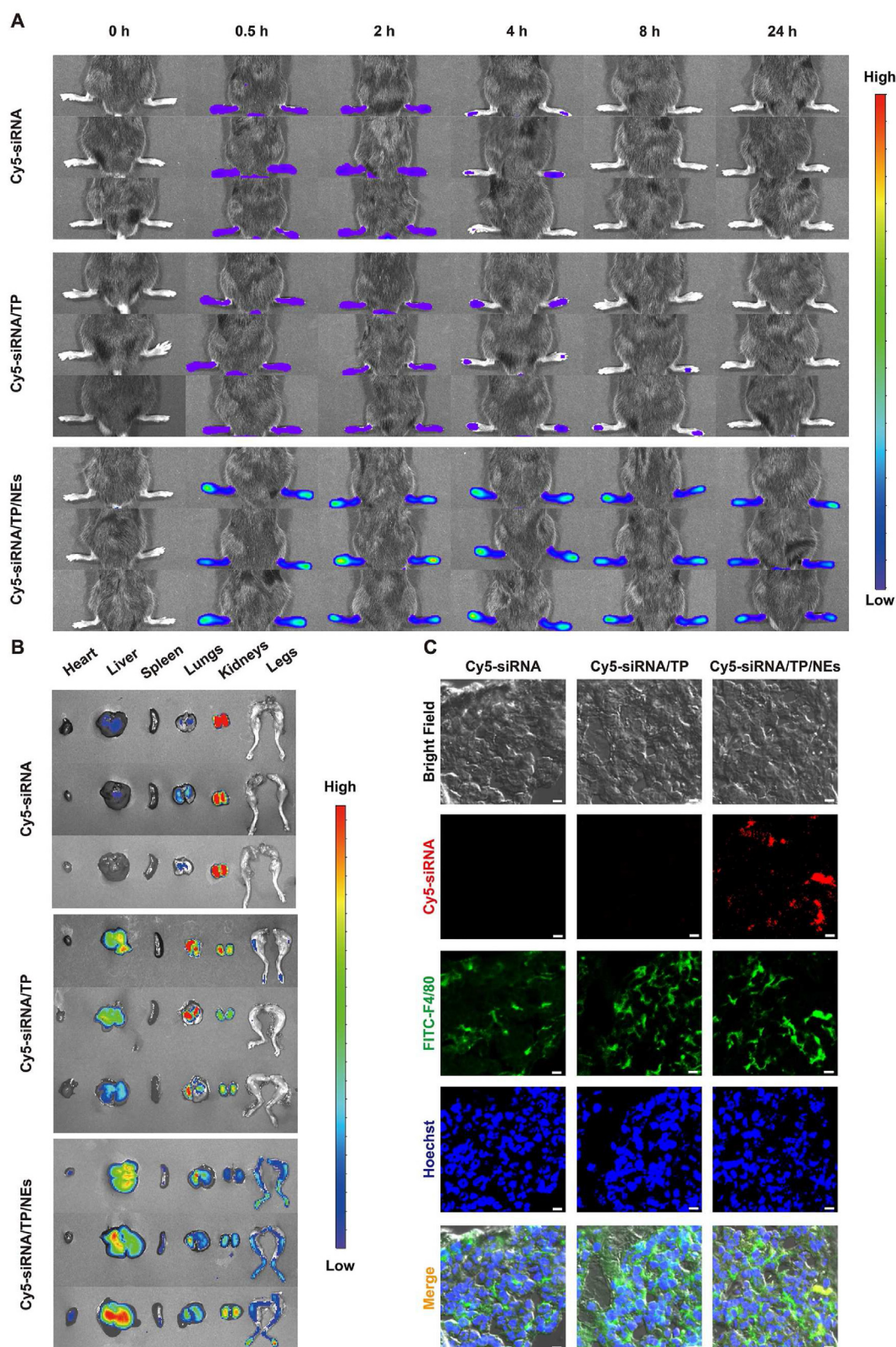


Figure 5 The biodistribution of Cy5-siRNA/TP/NEs *in vivo*. (A) *In vivo* images of arthritic joints over time after intravenous injection of free Cy5-siRNA, Cy5-siRNA/TP or Cy5-siRNA/TP/NEs into CIA mice, at a dose of 0.3 mg/kg, respectively. (B) Accumulation of Cy5-siRNA in the joints and different organs detected using the *ex vivo* imaging at 24 h post-injection of different formulations. (C) Frozen sections of synovium to observe the cellular distribution of Cy5-siRNA. Macrophages were marked by F4/80-FITC (Green) and nucleus was stained by Hoechst 33342 (Blue). Scale bar: 5 μ m.

siRNA and Cy5-siRNA/TP showed a low level of Cy5 fluorescence in paws after 0.5 h, which could be ascribed to the quickly elimination of free siRNA through kidney as well as the insufficient targeting and retention ability of nanoparticles in inflamed joint. The *ex vivo* images of major organs (*e.g.*, heart, liver, spleen, lungs, kidneys and legs) of mice after treatment of 24 h further indicated the sustained targeting and retention ability of reprogrammed siRNA/neutrophil cytopharmaceuticals (Fig. 5B).

Further, we explored the *in vivo* uptake of reprogrammed siRNA/neutrophil cytopharmaceuticals by macrophages. The dissected synovium tissue of each group was sliced and stained with F4/80, a typical marker of macrophages, which was then observed by CLSM. Compared to the free Cy5-siRNA and Cy5-siRNA/TP treated mice, Cy5-siRNA/TP/NEs treated mice exhibited the brightest red fluorescence in the synovium, which was also co-localized with the FITC-F4/80 immunofluorescence (Fig. 5C), indicating that the siRNA accumulated in the synovium was mainly uptake by macrophages. All results above suggest that the reprogrammed siRNA/neutrophil cytopharmaceuticals had excellent joint accumulation, improved synovium retention, and efficient macrophage targeting capabilities, which might result in a promising RA treatment.

3.5. *In vivo* therapeutic efficacy and safety assay of siTNF α /TP/NEs

Finally, we investigated the therapeutic efficacy of the reprogrammed siRNA/neutrophil cytopharmaceuticals in CIA mice following the treatment scheme (Fig. 6A). Twenty-one days after the first immunization, mice were received the second immunization and then randomly divided into 5 groups ($n = 5$ in each group), which were intravenously injected with saline, siNC/TP/NEs (0.3 mg/kg), siTNF α /TP (0.3 mg/kg), free MTX as a positive control (0.75 mg/kg), and siTNF α /TP/NEs (0.3 mg/kg), respectively. The normal mice were used as the negative control. All the groups were treated every 3 days for eight times. The arthritis severity was scored every 3 days since Day 21 following a clinical scoring system which assesses the degree of paw swelling and redness. As shown in Fig. 6B, the arthritis score of paws rapidly increased in saline-, siTNF α /TP- and siNC/TP/NEs-injected mice with uncontrolled disease progression, while that of free MTX and siTNF α /TP/NEs groups were significantly slowed down even to 49 days. The paw thickness was also measured to evaluate the paw swelling of CIA mice (Fig. 6C), which showed a similar tendency with the arthritis scores. These results indicate the markedly relieved RA inflammation in the mice treated with MTX and siTNF α /TP/NEs. Of which, siTNF α /TP/NEs showed a mild improved efficacy with the commercially available drug MTX.

In order to elucidate the direct effect of siTNF α on its target, we used ELISA assay to measure the TNF α protein in sera (Fig. 6D). Among the treated groups, siTNF α /TP/NEs exhibited the lowest TNF α level, indicating the successful *in vivo* gene silencing of siTNF α /TP/NEs, which was ascribed to the collected merits of neutrophil targeting ability and effective siRNA transfer to macrophages in RA joint. Moreover, the mRNA levels of cytokines related to RA including *Tnfa*, *Adamts5* and *Mmp13* in CIA mice joints were also tested. As expected, siTNF α /TP/NEs treated mice significantly reduced the mRNA levels of *Tnfa* (Fig. 6E), *Adamts5* (Fig. 6F), and *Mmp13* (Fig. 6G), while the unprogrammed neutrophils significantly induced these mRNA levels.

We further accessed the relative protein expression in the synovium and cartilage by immunohistochemical staining (Supporting Information Fig. S14). Compared with saline group, siTNF α /TP/NEs treatment significantly reduced the protein levels of TNF α , ADAMTS5 and MMP13 of about 60%, 75%, and 72%, respectively, which were consistent with the q-PCR results.

The therapeutic efficacy was further evaluated by magnetic resonance imaging (MRI) and histological analysis with hematoxylin-eosin staining (H&E). MRI can simultaneously assess the pathological functions and anatomical structure in the inflamed joints and has been widely used for clinical RA assessment post-treatments⁴³. Here, we used T2-weighted signals to observe the inflamed joints (Fig. 7A). The inflammation site with brightness indicated by white arrowheads displayed that mice injected with siTNF α /TP/NEs possessed efficiently alleviative inflammation, whereas injected with saline, siTNF α /TP and siNC/TP/NEs still maintained severe inflammation, and with MTX showed mild inflammation. The H&E staining of joint sections which isolated from CIA mice received siTNF α /TP/NEs administration showed smooth and integrity cartilage zone (Fig. 7B), confirming the effective cartilage protection of reprogrammed siRNA/neutrophil cytopharmaceuticals in RA treatment. In contrast, the saline, siTNF α /TP and siNC/TP/NEs groups presented rough and irregular patterns (Fig. 7B), indicating the impaired cartilage tissues due to the RA progress, as well as the ineffectiveness of less targeted siTNF α /TP and unprogrammed siNC/TP/NEs. Despite the improved curative effect of MTX, the rough cartilage zone implied the insufficient cartilage protection (Fig. 7B). To detailed access the cartilage protection of siTNF α /TP/NEs, micro-CT analysis (Fig. 7C) and safranin O-fast green staining (Fig. 7D) were proceeded. We found that, in contrast with the rough bone surface and serious bone erosion in the knee joints of saline-treated mice, siTNF α /TP/NEs group displayed smooth bone surface and attenuated osteophytosis which was better than other formulations. Similarly, safranin O-fast green staining showed that the thickness of the proteoglycans in siTNF α /TP/NEs group resembled to that of normal group, indicating a distinguished cartilage protection, whereas other groups held significantly thinner proteoglycans.

In vivo safety of siTNF α /TP/NEs should also be take concerns for the future application of siTNF α /TP/NEs in RA treatment. For this purpose, we performed histopathological analysis of major organs including heart, liver, spleen, lungs and kidneys extracted from CIA mice receiving different formulations. H&E staining suggested that no significant tissue toxicity was found among all the groups (Supporting Information Fig. S15A). Moreover, the body weights of each group exhibited no obvious variation over time (Fig. S15B). The biochemical indexes of the liver (Alanine transaminase, ALT; aspartate transaminase, AST), and renal (Blood urea nitrogen, BUN; creatinine, CRE; uric acid, UA) in CIA mice treated with siTNF α /TP/NEs showed no significant changes with normal mice, demonstrating that siTNF α /TP/NEs had no harmful to the liver and kidney function of CIA mice (Fig. S15C–S15G). These results further confirm the well tolerance of siTNF α /TP/NEs.

Taken together, we have demonstrated that the safe reprogrammed siRNA/neutrophil cytopharmaceuticals hold the potent potential in RA treatment through effective inhibiting the production of inflammatory factor TNF α by macrophages and destroying the related inflammatory network, thus leading to the alleviate synovial inflammation and improved cartilage protection.

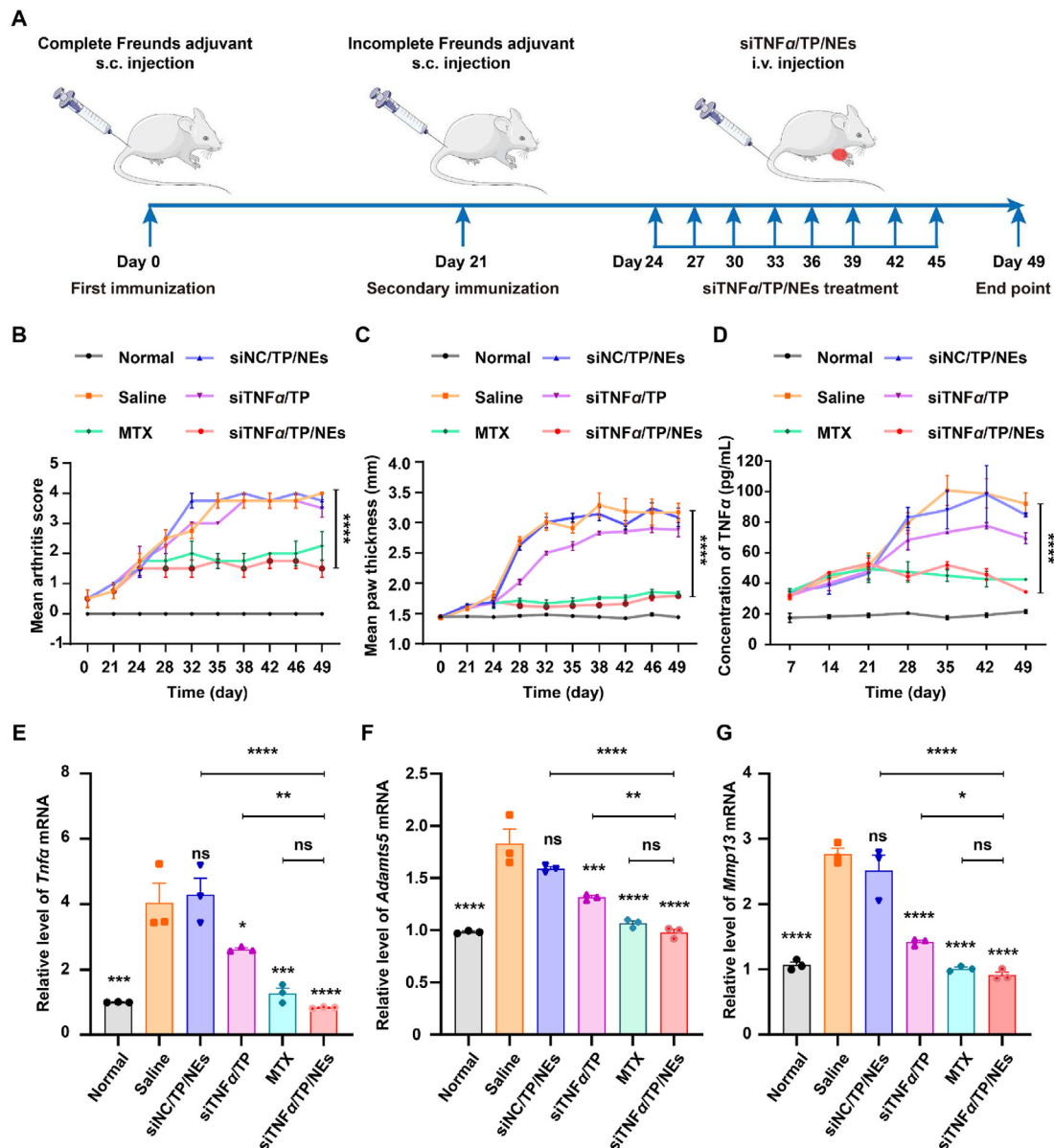


Figure 6 Evaluation of the *in vivo* anti-rheumatoid arthritis effect mediated by siTNFα/TP/NEs. (A) Schematic illustration of the administration regimen. On Day 0, mice were subcutaneously injected (s.c.) with complete Freund's adjuvant in the skin of the tail at the base of the tail. After 21 days, mice were subcutaneously injected with incomplete Freund's adjuvant in the skin of the tail at the base of the tail as the second immunization. Next, the CIA mice were intravenously injected (i.v.) with saline, siNC/TP/NEs, siTNFα/TP, free MTX, and siTNFα/TP/NEs every 3 days for eight times. (B) Arthritic score measurement in CIA mice after different treatment over time. (C) Thickness of paws of CIA mice after different treatment over time. (D) Concentration of TNFα protein in the serum of CIA mice after different treatment over time. Relative mRNA levels of (E) *Tnfα*, (F) *Adamts5*, and (G) *Mmp13* in the joints of CIA mice after different treatment. The data at different groups ($n = 3$) were shown as mean \pm SEM and analyzed by one-way ANOVA with Turkey's correction. Compared to Saline group: ns, not significant, $*P < 0.05$, $***P < 0.001$, $****P < 0.0001$. The significance of pairwise group is shown on the top of the corresponding line. ns, not significant, $\#P < 0.05$, $##P < 0.01$, $###P < 0.0001$.

4. Discussion

In this study, we have developed reprogrammed siTNFα/neutrophil cytopharmaceuticals for RA treatment. Unlike the traditional drug such as MTX, reprogrammed siTNFα/neutrophil cytopharmaceuticals combine the merits of gene therapy and cell-based carrier, which have demonstrated their potential as an alternative anti-inflammatory approach for RA management.

Firstly, the delivery of gene drug like siTNFα to inflamed joints requires safe and efficient drug vectors. Conventional nanodrug carriers selectively accumulate and release drugs in the synovial tissue through the "ELVIS" (Extravasation through leaky vasculature and the subsequent inflammatory cell-mediated sequestration) effect^{44,45}. Whereas cell-based carriers possess unique chemotaxis to specific tissues and can bypass various biological/pathological barriers³³, which could further enhance the

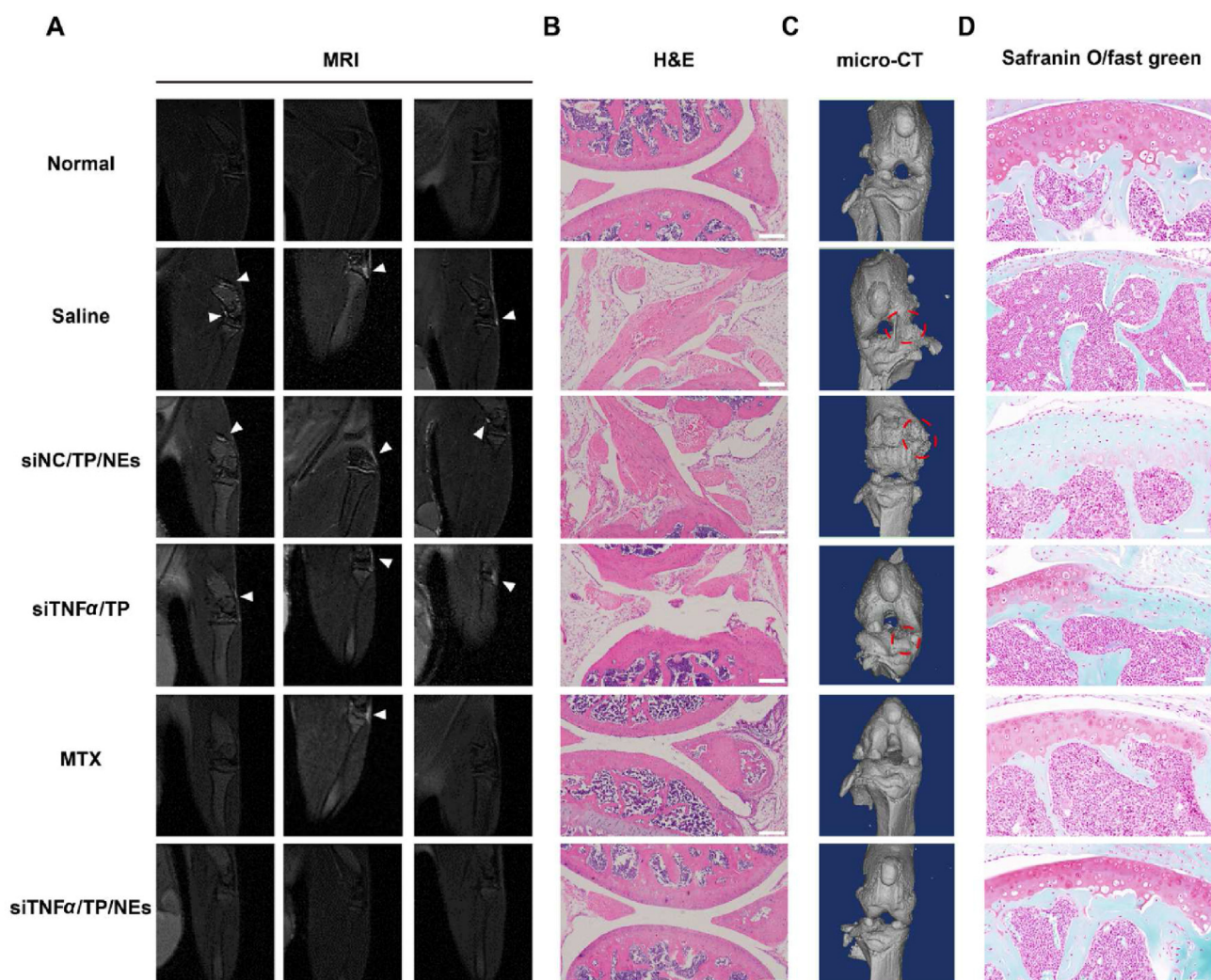


Figure 7 The MRI, H&E-stained images, micro-CT, and safranin O-fast green stained images of joint tissues of normal mice and saline, siNC/TP/NEs, siTNF α /TP, MTX and siTNF α /TP/NEs treated-CIA mice. (A) T2-weighted far-suppressed MRI images of arthritic joints. White arrows indicate the inflammation site of synovitis. (B) Histological analysis by H&E staining of joint tissue sections. Scale bar: 100 μ m. (C) Representative micro-CT images of arthritic joints. The red circles indicate periarticular osteophytes. (D) Proteoglycans assay by Safranin O-fast green staining of joint tissue sections. Scale bar: 50 μ m.

drug accumulation and retention in specific site. Especially, neutrophils exhibit an active tendency to inflammatory synovial tissue, rendering them suitable to act as an effective gene drug carrier for RA therapy. Here, we demonstrated that neutrophils could successfully deliver the loading siTNF α to the inflamed joints, and even the macrophages in inflammatory synovium. The dual-protected siTNF α /TP was fabricated through protamine condensation and TA7 cationic liposomes encapsulation to improve the stability of siTNF α within neutrophils. The chosen TA7 cationic liposomes cannot only load siTNF α /Prot in the cavity of liposomes to retard the degradation of enzymes, but also improve the cell uptake by neutrophils due to the positive charge³³ and promote the endo/lysosomal escape from neutrophils or macrophages owing to the proton buffering capacity of TA7³⁷. The loading process had no effect on the chemotaxis of neutrophils to inflammatory site. The transfer mechanism of siTNF α /TP from siTNF α /TP/NEs to macrophages was also explored. In the inflammatory environment, the upregulated inflammatory cytokines excessive activated the neutrophils to form the NETs to

render a concomitant release of siTNF α /TP which was then phagocytosed by macrophages. Besides, we found that the macrophages could engulf the apoptotic siTNF α /TP/NEs entirely, which might be an alternative transfer mechanism. Moreover, inflammatory macrophages might convert to the anti-inflammatory phenotypes due to the phagocytosis of apoptotic neutrophils³¹, which would be further confirmed in the future. In a word, the effective deliver of siTNF α to macrophages by neutrophil-based carriers guaranteed the anti-inflammatory effect through TNF α inhibition.

However, neutrophils themselves hold two facets in RA advancement. On one hand, they can release the microvesicles with annexin A1 (AnxA1) expression to protect the cartilage¹⁹, and their membrane can neutralize the inflammatory factors to alleviate the synovial inflammation²⁰. On another hand, neutrophils are capable of releasing the inflammatory factors such as TNF α to aggravate the synovial inflammation^{19,22}. The perpetuated inflammation would lead to the cartilage damage. Therefore, application of unprogrammed neutrophils as drug vectors faces the risk of promoting RA

progression. To avoid this, we assumed to reprogram neutrophils by the siTNF α /TP to silence the TNF α production by neutrophils. We demonstrated that the loaded siTNF α within neutrophils played the role in inhibiting TNF α expression over time. The probably reason might be that part of siTNF α /TP took actions in neutrophils. Moreover, the increased TGF- β levels and the inhibited MMP-9 expressions further demonstrated that the reprogramming by siTNF α could regulate neutrophils to be anti-inflammatory, which might circumvent the harmful effect of neutrophils in RA therapy. Beneficially, the significant reduced TNF α expression led to the down-regulation of ADAMTS5 and MMP13 in chondrocytes, thus exhibiting effective cartilage protection. These results suggested that reprogrammed neutrophils exhibited anti-inflammatory effect while kept the chemotaxis to inflamed joints, which adopted their good points of active targeting ability and avoid the shortcomings of RA promotion, implying a superior siRNA delivery vector in RA treatment.

Despite the improved RA therapy obtained by reprogrammed siTNF α /neutrophil cytopharmaceuticals, inhibition of TNF α alone might achieves insufficient curative effect since the pathogenesis of RA involves a complex network of various cytokines⁴⁶. Although neutrophil membrane can neutralize the detrimental inflammatory factors to some extent, it still encourages the future prospect of using multiple siRNA to inhibit RA related cytokines with the help of neutrophil-based vectors to achieve an persist efficacy on RA.

5. Conclusions

The reprogrammed siTNF α /neutrophil cytopharmaceuticals which fabricated by encapsulating siTNF α /TP to gain an anti-inflammatory neutrophil carrier, can target to the inflamed joints, prolong the residence time of siTNF α , transfer siTNF α to macrophages, and successfully reduce the TNF α production by macrophages and neutrophils, thus resulting in relived synovial inflammation and improved cartilage protection. This study provides an alternative anti-inflammatory gene therapy strategy for RA treatment, and puts forwards a siRNA delivery platform for inflammation-related diseases.

Acknowledgments

This work was supported by the National Natural Science Foundation of China (81930099, 82073785, 82130102, 92159304, 81773664), the Natural Science Foundation of Jiangsu Province (BK20212011, China), "Double First-Class" University project (CPU2018GY47, China), 111 Project from the Ministry of Education of China and the State Administration of Foreign Expert Affairs of China (No. 111-2-07, B17047, China), and the Open Project of State Key Laboratory of Natural Medicines (No. SKLNMZZ202223, China).

Author contributions

Yijun Chen designed and conducted all experiments, analyzed the data and wrote the manuscript. Kaiming Li designed and assisted in the cellular experiments. Mengying Jiao designed and assisted in all animal experiments, analyzed the data and wrote the manuscript. Yingshuang Huang assisted the animal experiments. Zihao Zhang synthesized the cationic lipid. Caoyun Ju supervised

all experiments and assisted in writing the manuscript. Can Zhang conceived the project and supervised all experiments. All of the authors have read and approved the final manuscript.

Conflicts of interest

The authors have no conflicts of interest to declare.

Appendix A. Supporting information

Supporting data to this article can be found online at <https://doi.org/10.1016/j.apsb.2022.08.012>.

References

- Gibofsky A. Overview of epidemiology, pathophysiology, and diagnosis of rheumatoid arthritis. *Am J Manag Care* 2012;**18**:295–302.
- Smolen JS, Aletaha D, Barton A, Burmester GR, Emery P, Firestein GS, et al. Rheumatoid arthritis. *Nat Rev Dis Prim* 2018;**4**: 18001–13.
- Guo Q, Wang YX, Xu D, Nossent J, Pavlos NJ, Xu J. Rheumatoid arthritis: pathological mechanisms and modern pharmacologic therapies. *Bone Res* 2018;**6**:1–14.
- Smolen JS, Landewe R, Bijlsma J, Burmester G, Chatzidionysiou K, Dougados M, Nam J, et al. Eular recommendations for the management of rheumatoid arthritis with synthetic and biological disease-modifying antirheumatic drugs: 2016 update. *Ann Rheum Dis* 2017;**76**:960–78.
- McInnes IB, Schett G. Cytokines in the pathogenesis of rheumatoid arthritis. *Nat Rev Immunol* 2007;**7**:429–42.
- Kinne RW, Brauer R, Stuhlmüller B, Palombo-Kinne E, Burmester GR. Macrophages in rheumatoid arthritis. *Arthritis Res Ther* 2000;**2**:189–202.
- Mix KS, Burrage PS, Brinckerhoff CE. Matrix metalloproteinases: role in arthritis. *Front Biosci* 2006;**11**:529–43.
- Schett G, Elewaut D, McInnes IB, Dayer JM, Neurath MF. How cytokine networks fuel inflammation: toward a cytokine-based disease taxonomy. *Nat Med* 2013;**19**:822–4.
- Nagy G, van Vollenhoven RF. Sustained biologic-free and drug-free remission in rheumatoid arthritis, where are we now? *Arthritis Res Ther* 2015;**17**:181–93.
- Baker KF, Skelton AJ, Lendrem DW, Scadeng A, Thompson B, Pratt AG. Predicting drug-free remission in rheumatoid arthritis: a prospective interventional cohort study. *J Autoimmun* 2019;**105**: 102298–310.
- Song Y, Jo S, Chung JY, Oh Y, Yoon S, Lee YL, et al. RNA interference-mediated suppression of TNF- α converting enzyme as an alternative anti-TNF- α therapy for rheumatoid arthritis. *J Control Release* 2021;**330**:1300–12.
- Smolen JS, Breedveld FC, Burmester GR, Bykerk V, Dougados M, Emery P, et al. Treating rheumatoid arthritis to target: 2014 update of the recommendations of an international task force. *Ann Rheum Dis* 2016;**75**:3–15.
- Choi HK, Hernan MA, Seeger JD, Robins JM, Wolfe F. Methotrexate and mortality in patients with rheumatoid arthritis: a prospective study. *Lancet* 2002;**359**:1173–7.
- Wang X, Yan X, Wang F, Ge F, Li Z. Role of methotrexate chronotherapy in collagen-induced rheumatoid arthritis in rats. *Z Rheumatol* 2018;**77**:249–55.
- Chan ES, Cronstein BN. Molecular action of methotrexate in inflammatory diseases. *Arthritis Res Ther* 2002;**4**:266–73.
- Braun J, Rau R. An update on methotrexate. *Curr Opin Rheumatol* 2009;**21**:36–49.
- Burn GL, Foti A, Marsman G, Patel DF, Zychlinsky A. The neutrophil. *Immunity* 2021;**54**:1377–91.

18. Phillipson M, Kubes P. The neutrophil in vascular inflammation. *Nat Med* 2011;**17**:1381–90.
19. Headland SE, Jones HR, Norling LV, Kim A, Souza PR, Corsiero E, et al. Neutrophil-derived microvesicles enter cartilage and protect the joint in inflammatory arthritis. *Sci Transl Med* 2015;**7**:190–218.
20. Zhang QZ, Dehaini D, Zhang Y, Zhou JL, Chen XY, Zhang LF, et al. Neutrophil membrane-coated nanoparticles inhibit synovial inflammation and alleviate joint damage in inflammatory arthritis. *Nat Nanotechnol* 2018;**13**:1182–90.
21. Mantovani A, Cassatella MA, Costantini C, Jaillon S. Neutrophils in the activation and regulation of innate and adaptive immunity. *Nat Rev Immunol* 2011;**11**:519–31.
22. Parsonage G, Filer A, Bik M, Hardie D, Lax S, Howlett K, et al. Prolonged, granulocyte–macrophage colony-stimulating factor-dependent, neutrophil survival following rheumatoid synovial fibroblast activation by IL-17 and TNF α . *Arthritis Res Ther* 2008;**10**:47–59.
23. Saw PE, Song EW. siRNA therapeutics: a clinical reality. *Sci China Life Sci* 2020;**63**:485–500.
24. Khoury M, Louis-Plence P, Escriviou V, Noel D, Largeau C, Cantos C, et al. Efficient new cationic liposome formulation for systemic delivery of small interfering RNA silencing tumor necrosis factor α in experimental arthritis. *Arthritis Rheumatol* 2006;**54**:1867–77.
25. Lee SJ, Lee A, Hwang SR, Park JS, Jang J, Huh MS, et al. TNF- α gene silencing using polymerized siRNA/thiolated glycol chitosan nanoparticles for rheumatoid arthritis. *Mol Ther* 2014;**22**:397–408.
26. Li J, Chen L, Xu XY, Fan Y, Xue X, Shen MW. Targeted combination of antioxidative and anti-inflammatory therapy of rheumatoid arthritis using multifunctional dendrimer-entrapped gold nanoparticles as a platform. *Small* 2020;**16**:2005661–78.
27. Aldayel AM, O'Mary HL, Valdes SA, Li X, Thakkar SG, Mustafa BE, et al. Lipid nanoparticles with minimum burst release of TNF- α siRNA show strong activity against rheumatoid arthritis unresponsive to methotrexate. *J Control Release* 2018;**283**:280–9.
28. Kanasty R, Dorkin JR, Vegas A, Anderson D. Delivery materials for siRNA therapeutics. *Nat Mater* 2013;**12**:967–77.
29. Whitehead KA, Langer R, Anderson DG. Knocking down barriers: advances in siRNA delivery. *Nat Rev Drug Discov* 2009;**8**:129–38.
30. Castanotto D, Rossi JJ. The promises and pitfalls of RNA-interference-based therapeutics. *Nature* 2009;**457**:426–33.
31. Fox S, Leitch AE, Duffin R, Haslett C, Rossi AG. Neutrophil apoptosis: relevance to the innate immune response and inflammatory disease. *J Innate Immun* 2010;**2**:216–27.
32. Alshaer W, Hillaireau H, Vergnaud J, Mura S, Delomenie C, Sauvage F, et al. Aptamer-guided siRNA-loaded nanomedicines for systemic gene silencing in CD-44 expressing murine triple-negative breast cancer model. *J Control Release* 2018;**271**:98–106.
33. Xue JW, Zhao ZK, Zhang L, Xue LJ, Shen SY, Wen YJ. Neutrophil-mediated anticancer drug delivery for suppression of postoperative malignant glioma recurrence. *Nat Nanotechnol* 2017;**12**:692–700.
34. Li YY, Hu QF, Li WS, Liu SJ, Li KM, Liu XWT, Du JJ, et al. Simultaneous blockage of contextual TGF- β by cyto-pharmaceuticals to suppress breast cancer metastasis. *J Control Release* 2021;**336**:40–53.
35. Wang F, Luo AS, Xuan WH, Qi L, Wu Q, Gan K, et al. The bone marrow edema links to an osteoclastic environment and precedes synovitis during the development of collagen induced arthritis. *Front Immunol* 2019;**10**:884–95.
36. Erdem-Cakmak F, Ozbas-Turan S, Salva E, Akbuga J. Comparison of VEGF gene silencing efficiencies of chitosan and protamine complexes containing shRNA. *Cell Biol Int* 2014;**38**:1260–70.
37. Lin ZM, Bao M, Yu ZX, Xue LJ, Ju CY, Zhang C. The development of tertiary amine cationic lipids for safe and efficient siRNA delivery. *Biomater Sci* 2019;**7**:2777–92.
38. Du JJ, Wang C, Chen YJ, Zhong LY, Liu XWT, Xue LJ, et al. Targeted downregulation of HIF-1 α for restraining circulating tumor micro-emboli mediated metastasis. *J Control Release* 2022;**343**:457–68.
39. Ju CY, Wen YJ, Zhang LP, Wang QQ, Xue LJ, Shen J, et al. Neo-adjuvant chemotherapy based on abraxane/human neutrophils cytopharmaceuticals with radiotherapy for gastric cancer. *Small* 2019;**15**:1804191–202.
40. Wright HL, Moots RJ, Edwards SW. The multifactorial role of neutrophils in rheumatoid arthritis. *Nat Rev Rheumatol* 2014;**10**:593–601.
41. van Zandbergen G, Klinger M, Mueller A, Dannenberg S, Gebert A, Solbach W, et al. Cutting edge: neutrophil granulocyte serves as a vector for entry into macrophages. *J Immunol* 2004;**173**:6521–33.
42. Scannell M, Flanagan MB, deStefani A, Wynne KJ, Cagney G, Godson C, et al. Annexin-I and peptide derivatives are released by apoptotic cells and stimulate phagocytosis of apoptotic neutrophils by macrophages. *J Immunol* 2007;**178**:4595–605.
43. Tamai M, Arima K, Nakashima Y, Kita J, Umeda M, Fukui S, et al. Fri0048 MRI bone erosion at baseline predicts the subsequent radiographic progression in early-stage RA patients who achieved in sustained clinical good response: sub-analysis from nagasaki university early arthritis cohort. *Ann Rheum Dis* 2015;**74**:436–43.
44. An LM, Li ZR, Shi LQ, Wang LJ, Wang Y, Jin L, et al. Inflammation-targeted celastrol nanodrug attenuates collagen-induced arthritis through NF- κ B and Notch1 pathways. *Nano Lett* 2020;**20**:7728–36.
45. Gai WW, Hao XF, Zhao JD, Wang LN, Liu JH, Jiang HX, et al. Delivery of benzoyleconitine using biodegradable nanoparticles to suppress inflammation via regulating NF- κ B signaling. *Colloids Surf, B* 2020;**191**:110980–90.
46. Kondo N, Kuroda T, Kobayashi D. Cytokine networks in the pathogenesis of rheumatoid arthritis. *Int J Mol Sci* 2021;**22**:10922–34.